Adversarial Audit of the "Native Many-Body Shared-Register" Benchmark

Independent technical review

June 2026

Abstract

The numerical outputs of the native shared-register package reproduce, but its central interpretation does not. The large-size calculation is a four-dimensional momentum-space ansatz whose power laws are fixed algebraically by inserted factors of k^r; it is not a local many-body simulation of a flavored $U(2) \to SU(2)$ link lattice coupled to a six-component tensor register. Two new real-space tests show why this distinction matters. A fixed local two-derivative gauge-breaking interaction in the previously constructed six-state flavored-link chain leaves a nonzero Gauss-defect density as L grows, and a quadratic tensor model has a soft-mode defect weight proportional to L^{-4} while its integrated defect density approaches a nonzero constant. Curvature filtering can improve long-wavelength Ward diagnostics without dynamically selecting the exact constraint sector.

1 Verdict

The original values and plots are numerically reproducible. The claimed "positive many-body mechanism," however, is not established. The defensible result is narrower:

> If the microscopic model is *assumed* to contain only a two-derivative physical–defect vertex, then the selected lowest-momentum mode has defect amplitude proportional to k^2. This does not imply that the local many-body defect density vanishes at fixed finite penalty.

2 Why the reported exponents are predetermined

The large-L scan diagonalizes

$$H(k) = \begin{pmatrix} ck & gk^2 & \epsilon_T k^r & 0 \\ gk^2 & \sqrt{\Delta_S^2 + v_S^2 k^2} & 0 & \epsilon_G k^r \\ \epsilon_T k^r & 0 & \Delta_T + O(k) & 0 \\ 0 & \epsilon_G k^r & 0 & \Delta_G + O(k) \end{pmatrix}, \qquad k = 2\sin\frac{\pi}{L}. \tag{1}$$

For nonzero gaps, ordinary nondegenerate perturbation theory gives

$$P_T^{\mathrm{def}} = \frac{\epsilon_T^2}{\Delta_T^2} k^{2r} + o(k^{2r}), \tag{2}$$

$$P_S = \frac{g^2}{\Delta_S^2} k^4 + o(k^4), \tag{3}$$

$$P_G^{\mathrm{def}} = \frac{g^2 \epsilon_G^2}{\Delta_S^2 \Delta_G^2} k^{2r+4} + o(k^{2r+4}), \tag{4}$$

$$W = \frac{|\epsilon_T|}{\Delta_T} k^r + o(k^r). \tag{5}$$

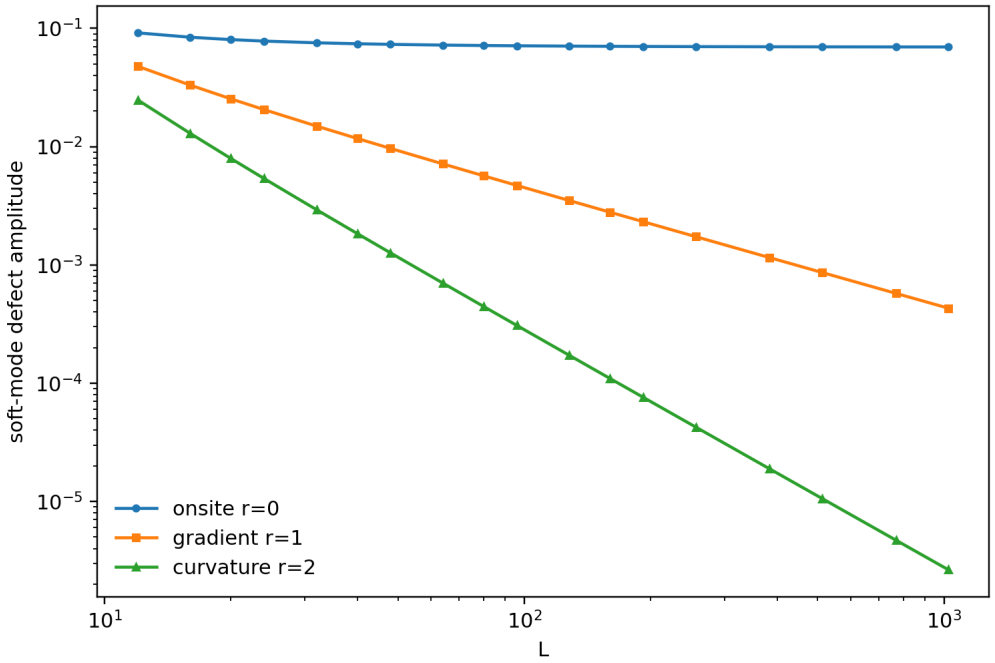

Figure 1: The soft-mode scaling is generated by the explicitly inserted powers k^r.

Since $k \sim 2\pi/L$, the $r = 2$ slopes are necessarily -4, -4, -8, and -2. At $L = 1024$, the numerical values divided by these leading expressions are respectively 1.0046, 1.0118, 1.0157, and 1.0023. The fit quality therefore confirms the implementation of the ansatz, not an emergent renormalization flow.

The onsite control has an additional problem. Its minimum one-particle eigenvalue becomes negative by $L = 1024$ and approaches about -9.7×10^{-3}. An unrestricted number-conserving bosonic second quantization of that matrix is then unbounded below, so it is not a stable many-body negative control without an additional occupation constraint or stabilizing interaction.

3 What the auxiliary audits do and do not prove

Square-root ladder. The Fock calculation correctly verifies the identity that the spectrum of $\mathrm{d}\Gamma(A)$ in the two-particle sector consists of pairwise sums of the eigenvalues of A. This is a valid audit of the $\sqrt{n+1}$ amplitudes. It does not validate the curvature scan: the real-space matrix used in the Fock test is gapped and has momentum-independent inter-channel couplings rather than the k^2 vertices used above.

Local $SU(2)$ singlet. The identity $[\mathbf{S}_0 \cdot \mathbf{S}_1, \mathbf{S}_0 + \mathbf{S}_1] = 0$ is exact, but it is not a lattice Gauss-law test involving colored links, neighboring vertices, mobile matter, or the flavored determinant operator.

Dressed constraints. The package defines $H = UH_0U^\dagger$ and $G_\mathrm{d} = UGU^\dagger$. Hence $[H, G_\mathrm{d}] = U[H_0, G]U^\dagger$ identically. This verifies basis covariance. It does not construct a Schrieffer–Wolff or quasi-adiabatic dressing for an independently specified perturbation, nor does it test the spatial decay of the dressed generator.

Pole separation. The continuum edge is stipulated as twice a chosen singlet dispersion. It is not extracted from the complete interacting spectrum, so the plotted separation is a property of the ansatz rather than a many-body pole theorem.

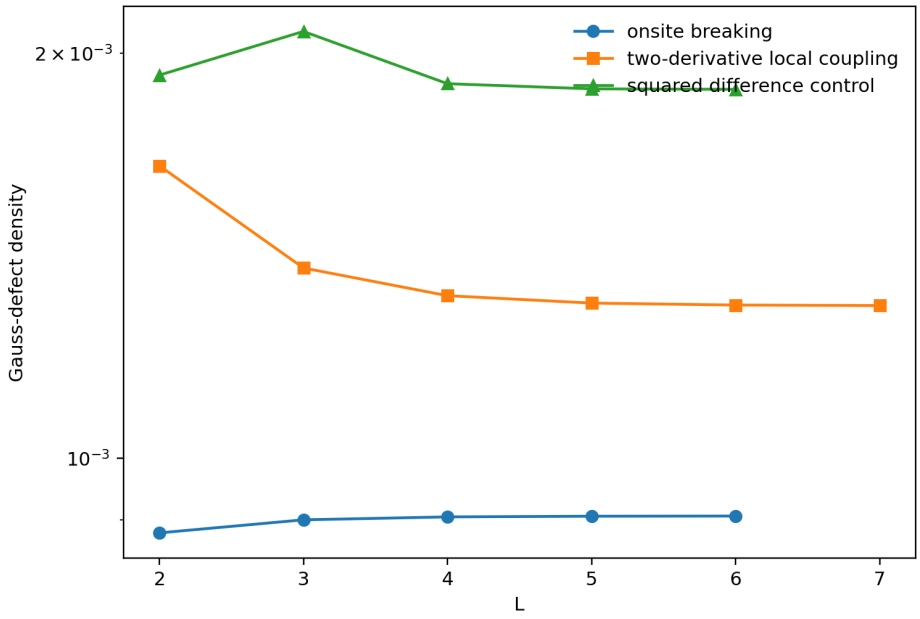

Figure 2: Exact-diagonalization results for the local flavored-link chain. Derivative filtering changes the floor but does not make the local defect density vanish.

4 New real-space flavored-link test

To test the claimed mechanism directly, we returned to the exact six-state flavored $U(2) \to SU(2)$ link register used in the earlier dynamical-selection calculation. The gauge-symmetric parent Hamiltonian was perturbed by the fixed local interaction

$$V_{\nabla^2} = \frac{\epsilon}{2} \sum_x \{B_{x+1} - B_x,\ E_{x+1} - E_x\}\,, \tag{6}$$

where B_x is the local gauge-breaking link operator and E_x is the color-singlet electric operator. Its long-wavelength vertex is proportional to k^2, but no parameter is retuned with L.

L	Hilbert dimension	ρ_G
2	36	1.64958×10^{-3}
3	216	1.38507×10^{-3}
4	1296	1.32098×10^{-3}
5	7776	1.30434×10^{-3}
6	46656	1.29999×10^{-3}
7	279936	1.29882×10^{-3}

Table 1: The local Gauss-defect density approaches a nonzero floor despite the two-derivative vertex.

At $L = 5$, varying ϵ gives

$$\rho_G \propto \epsilon^{2.00191}, \qquad R^2 = 0.99999965, \tag{7}$$

which is the expected finite-penalty virtual-defect law. The result is suppressed by increasing the Gauss penalty, not by increasing volume.

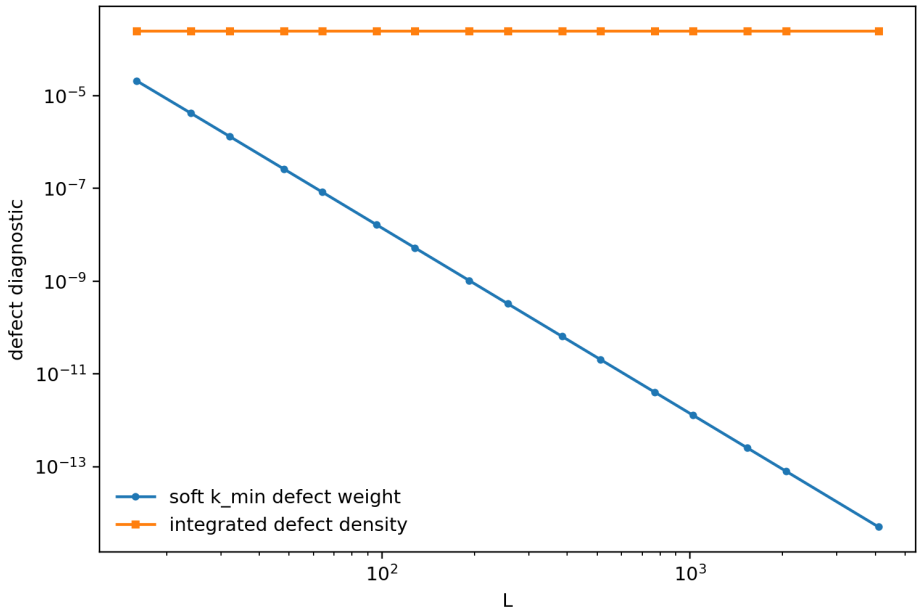

Figure 3: A closing $k_{\min}$ defect weight does not imply a vanishing integrated defect density.

5 Soft Ward improvement versus local tensor leakage

A second countertest uses a local quadratic oscillator model with one massless physical channel, one gapped defect channel, and a stiffness mixing proportional to $\widehat{k}^2$. The lowest-momentum eigenvector has

$$P_{\mathrm{def}}(k_{\min}) \propto L^{-3.99997}, \tag{8}$$

but the bare defect occupation summed over all lattice momenta approaches

$$\frac{1}{L}\sum_{k} n_{\mathrm{def}}(k) \longrightarrow 2.47126302554 \times 10^{-4}. \tag{9}$$

The ultraviolet part of the Brillouin zone leaves a finite local density even though the infrared mode becomes arbitrarily transverse.

6 Corrected status and next decisive test

The original package supports four limited statements: the numerical ansatz was implemented correctly; square-root ladders realize ordinary bosonic second quantization; a simple spin scalar is an $SU(2)$ singlet; and derivative vertices suppress a selected soft-mode admixture. It does not demonstrate dynamical selection of a shared exact $SU(2) + TT$ phase.

A decisive positive result requires one of two stronger mechanisms:

1. an exact microscopic joint constraint algebra, with every native update in its commutant; or
2. a quasi-local dressed algebra constructed from an independently specified perturbed many-body Hamiltonian.

For the second route, one must report the real-space support tails of the dressed generators, a volume-uniform defect gap, local defect densities, fixed-physical-momentum Ward correlators, and the interacting continuum edge from the same Hamiltonian. Defining a commuting dressed operator by diagonalizing a finite Hamiltonian is insufficient unless its quasi-locality and volume stability are demonstrated.

7 Conclusion

The latest positive claim should be withdrawn or rewritten as an effective infrared illustration. The new tests show that curvature filtering alone can protect long-wavelength response while leaving a finite density of local constraint violations. The earlier negative finite-penalty conclusion therefore remains the stronger many-body result.